Ocean Engineering 142 (2017) 616–624

Contents lists available at ScienceDirect

Ocean Engineering

journal homepage: www.elsevier.com/locate/oceaneng

A study on path optimization method of an unmanned surface vehicle under environmental loads using genetic algorithm

Heesu Kim[1], Sang-Hyun Kim[*,1], Maro Jeon[1], JaeHak Kim[1], Soonseok Song[1], Kwang-Jun Paik[1]

Inha University, 100, Inha-ro, Nam-gu, Incheon 402-751, Republic of Korea

ARTICLE INFO

Keywords:
Path optimization
Genetic algorithm
Environmental load
Fixed obstacle avoidance

ABSTRACT

Setting a path is essential for reaching a target point and avoiding obstacles in the autonomous navigation system for an unmanned surface vehicle (USV). Accordingly, a decision algorithm for determining an optimized path, considering ocean environmental loads, is necessary. In this study, a genetic algorithm was used to determine the optimized path with the minimum travel time for a USV under environmental loads. The optimized paths were determined using numerical simulations. First, the path of the vessel under environmental loads was expressed using chromosomes consisting of the turning angle of the vessel per unit time. In the configuration of the decision algorithm, the following three objective functions were derived: avoiding obstacles, reaching a target point, and minimizing travel time. By integrating the three objective functions, a new fitness function was proposed. In addition, to determine the optimized path, the fitness evaluation of each chromosome was repeated for all generations using the fitness function. Using the proposed algorithm, the optimized paths were determined considering environmental loads and the allowed minimum distance of approach to an obstacle, and validated using numerical simulations.

1. Introduction

Determining the route of an unmanned surface vehicle (USV) is an important problem associated with its safety and efficiency. According to the trends in ship automation systems and unmanned technology, an electronic navigation chart (ENC) has been introduced, and research on its application is being conducted actively. Accordingly, research is required to determine the route of a ship on an ENC. Lee et al. (2000) have discussed the necessity of this research. In addition, finding the best route autonomously is necessary to manage a USV effectively in a wide area. The necessity of the research is described by Kim et al. (2012).

However, autonomous path planning should consider overcoming environmental loads in real ocean environments, and minimizing energy consumption to maximize the capability of a USV's operations. This is why, even though the shortest path that avoids obstacles is planned, a USV cannot follow this path owing to a thrust limit.

A genetic algorithm, which is also referred to as an optimization algorithm, can search for an optimal solution robustly even if a problem is complex or if additional information is not provided. When various environmental loads are considered, the following difficulties are encountered while solving problems: lack of advanced information and limitations of functions in conjunction with a large search space. Thus, genetic algorithms could be suitable for searching for an optimized path and finding a valid solution. Lee et al. (2000) discussed the suitability of genetic algorithms for searching for an optimized path.

In this study, the optimized path of a USV, considering environmental loads, is found using a genetic algorithm. The following three objective functions are derived: avoiding obstacles, reaching a target point, and minimizing travel time. A new fitness function is proposed by integrating the three objective functions. An optimized path is found using evolutionary processes and repeating fitness evaluations of each chromosome over all generations using the fitness function. If the proposed algorithm is applied to search for paths, the optimized paths that have the minimum travel distance or time can be obtained. The proposed algorithm is verified using numerical simulations for several conditions of environmental loads and obstacles.

2. Genetic algorithm

A genetic algorithm is a stochastic searching method, which obtained its idea from the evolution of organisms. The algorithm is modeled using natural phenomena including genetic inheritance and Darwin's survival of the fittest. The structure of a genetic algorithm is shown in Fig. 1.

* Corresponding author.
E-mail address: kimsh@inha.ac.kr (S.-H. Kim).
[1] 22161413@inha.edu

http://dx.doi.org/10.1016/j.oceaneng.2017.07.040
Received 24 October 2016; Received in revised form 7 March 2017; Accepted 11 July 2017
Available online 21 July 2017
0029-8018/ © 2017 Elsevier Ltd. All rights reserved.

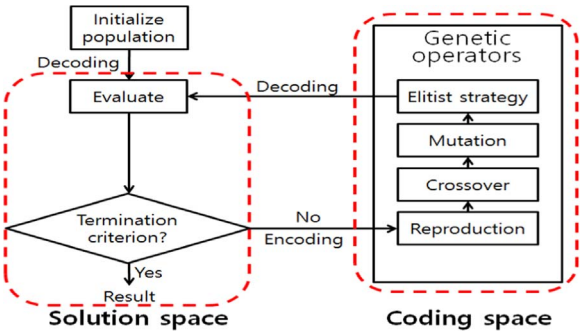

Fig. 1. Structure of genetic algorithm.

2.1. Initialization

In the initialization process, an initial population is generated, and a simulated evolution occurs. Random initialization, i.e., generating a population randomly, is used in this study. The process of random initialization is shown in Fig. 2. Random initialization is described by Jin (2010).

2.2. Fitness function evaluation

The fitness of every individual is evaluated over all newly generated populations in each generation. The fitness function is derived from the objective function, which is required for appropriate mapping, as follows:

$$f(s) = \frac{1}{F(x) + \gamma} \tag{1}$$

where $F(x)$ is the objective function, $f(s)$ is the fitness function, x is a multi-dimensional vector, s is a string vector or chromosome, and γ is a constant. The equation always satisfies $f(s) \geq 0$ (Jin, 2010).

2.3. Genetic operators

Genetic operators include reproduction, crossover, mutation, and elitist strategy. A reproduction operator selects individuals, which could be the source of a crossover, from the current population based on the fitness. A crossover operator creates a new chromosome by combining the characteristics of two other chromosomes. A mutation operator alters some genes in the chromosome from their initial state. In the elitist strategy, the best organism is carried over to the next generation, unaltered, by replacing the worst organism in the current generation (Jin, 2010).

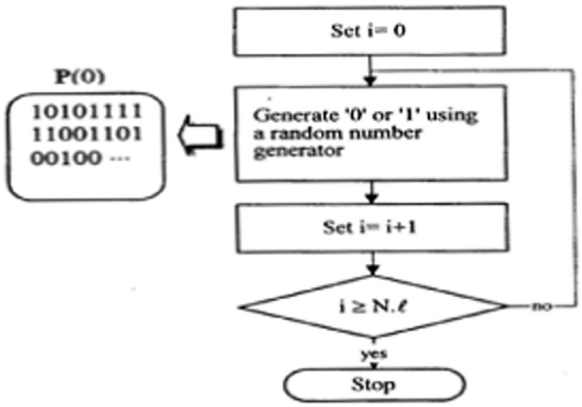

Fig. 2. Random initialization (Jin, 2010).

3. Genetic representation of a path of a ship

To apply the genetic algorithm to optimize the path of a ship, a genetic representation of the path is required. In addition, the fitness of the path must be evaluated using the fitness function.

Therefore, the turning angle of the ship per unit time is represented in the form of a chromosome, simplifying the motion of the ship. The moving distance of the ship per unit time is also calculated, considering the velocity induced by thrust, and the velocity variation induced by environmental loads. The path of the ship is expressed by combining the turning angle and the moving distance per unit time explained above.

3.1. Turning angle per unit time

The expression for the chromosome that represents the solution of a path, is

$$a^T = [a_1 a_2 a_3 \cdots a_n] \tag{2}$$

where a is turning angle, and n is the length of the chromosome. n is derived as follows:

$$n = \frac{t_0}{t_u} \tag{3}$$

where t_0 is the virtual operating time required to create the path of the ship, and t_u is the unit time during the turning movement. By following the notation of Lee et al. (2012), the path that is represented by the chromosome can be explained as shown in Fig. 3.

Here, $p_1, p_2, p_3, \cdots$ are the locations per unit time t_u, and p_n is the location at the final time t_0.

3.2. Moving distance per unit time

From Fig. 4, the velocity vector of the ship satisfies

$$\vec{U_i} = (\vec{V_t})_i + (\vec{V_e})_i \tag{4}$$

to move along the path line represented by the chromosome, where $\vec{U_i}$ is the velocity vector following the path line, $(\vec{V_t})_i$ is the velocity vector induced by the thrust of the ship, and $(\vec{V_e})_i$ is the velocity vector induced by the environmental loads on the ship. Hence, it follows that

$$(V_t)_i sin(\theta_t)_i = (V_e)_i sin(\theta_e)_i \tag{5}$$

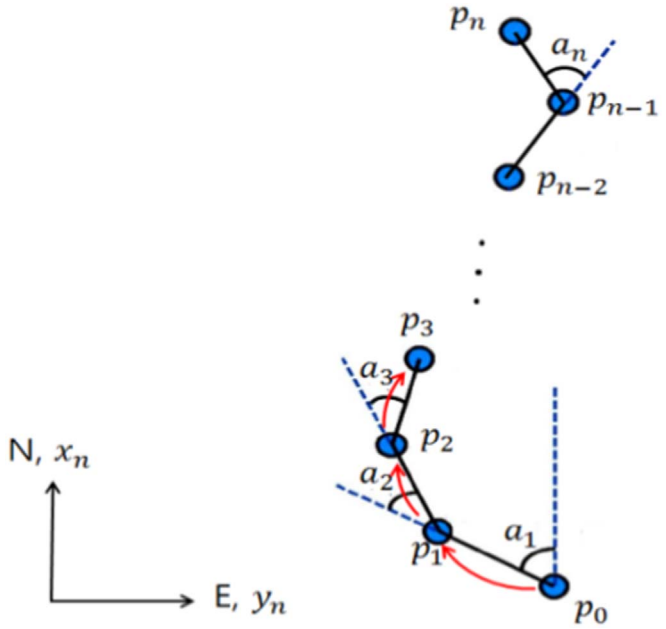

Fig. 3. Created path by a chromosome in North-East-Down coordinate system.

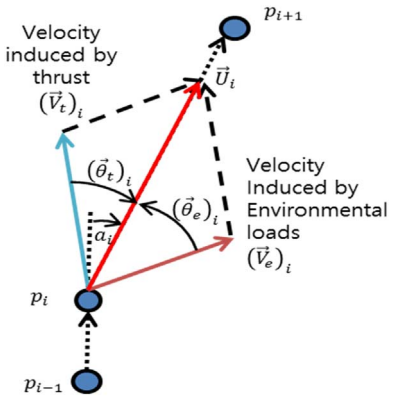

Fig. 4. Velocities of a ship induced by thrust and environmental loads.

where $(V_t)_i$ is the magnitude of the vector $(\vec{V_t})_i$, $(V_e)_i$ is the magnitude of the vector $(\vec{V_e})_i$, $(\theta_t)_i$ is the angle between the path line and $(\vec{V_t})_i$, and $(\theta_e)_i$ is the angle between the path line and $(\vec{V_e})_i$. In this study, it is assumed that the ship speed induced by the thrust and ship velocity vector induced by the environmental loads were provided. Thus, $(V_t)_i$, $(V_e)_i$, and $(\theta_e)_i$ were given in advance, and $(\theta_t)_i$ can be calculated using Eq. (5). Hence, the speed of the ship is

$$U_i = (V_t)_i cos(\theta_t)_i + (V_e)_i cos(\theta_e)_i \tag{6}$$

Thus, the moving distance of the ship, S_i, from p_i to p_{i+1}, becomes

$$S_i = U_i \times t_u \tag{7}$$

3.3. Path representation of a ship

Fig. 5 shows an example of the path that combines the turning angle and the moving distance from Eq. (2) and Eq. (7), respectively.

The paths are created randomly during the initialization of the genetic algorithm. The best path is selected using the operating procedures of fitness evaluation, reproduction, mutation, and elitist strategy.

4. Fitness function for searching for the best path

The fitness function is composed of the following three objective functions: reaching a target location point, avoiding obstacles, and minimizing travel time.

4.1. Determination of the last location point of a path

A location point, represented by p_i, can be defined as

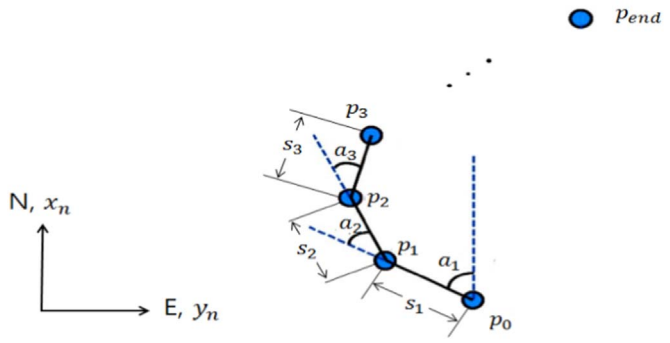

Fig. 5. Represented path of a ship.

for $i = 1$: end
  if $\|p_i - p_g\| \le \varepsilon$
    $p_i = p_{cut}$
  else
    $p_{end} = p_{cut}$
  end
end (8)

where p_i is the i^{th} location point, p_g is the target location point, p_{cut} is the last location point that is newly determined, and ε is the allowable distance error from the target location point (Lee et al., 2012). p_{cut} is set as the last location point, as shown in Fig. 6.

If the one of p_i is located in the range of ε, this p_i is set as p_{cut} as shown in Fig. 6(a). On the other hand, if any p_i are not located in the range of ε, the p_{end} is set as p_{cut} as shown in Fig. 6(b). The purpose of this process is to reduce computational demand as excluding the calculation of the points after p_{cut} if the path passes through the range of ε.

4.2. Objective function: reaching a target location point

Depending on whether or not the distance between the last location point and the target location point is within the allowable distance error, one of the objective functions, F_g, is defined as

if $\|p_{cut} - p_g\| \le \varepsilon$
  $F_g = 0$
else
  $F_g = \infty$ (9)

The cases for the abovementioned values of F_g are shown in Fig. 7.

Fig. 7(a) and (b) show the cases of that the F_g is set to 0 as the one of p_i is placed in the range of ε. On the contrary, Fig. 7(c) shows the case that the F_g is set to infinity as any points are not placed in the range of ε.

4.3. Objective function: avoiding obstacles

The second objective function, F_o, is defined as

for $i = 1$: cut
  for $j = 1$: k
    if $\|p_i - (p_o)_j\| > r_j$
      $F_o = 0$
    else
      $F_o = \infty$
    end
end (10)

Where cut is the index number of the last point as shown in Fig. 6, $(p_o)_j$ is the center location point of an obstacle, r_j is the radius of the obstacle, and k is the number of obstacles. The cases for the abovementioned values of F_o are shown in Fig. 8.

Fig. 8(a) shows the case of that the F_o is set to 0 as the any of p_i are not placed in the range of r_j. On the other hands, Fig. 8(b) and (c) show the cases that the F_o is set to infinity as the ones of the points are placed in the range of r_j.

4.4. Objective function: travel time

The third objective function, F_t, is defined as

$$F_t = t_u \times cut \tag{11}$$

where t_u is the travel time between each location point.

4.5. Fitness function

The final objective function value is defined as

$$F = F_g + F_o + F_t \tag{12}$$

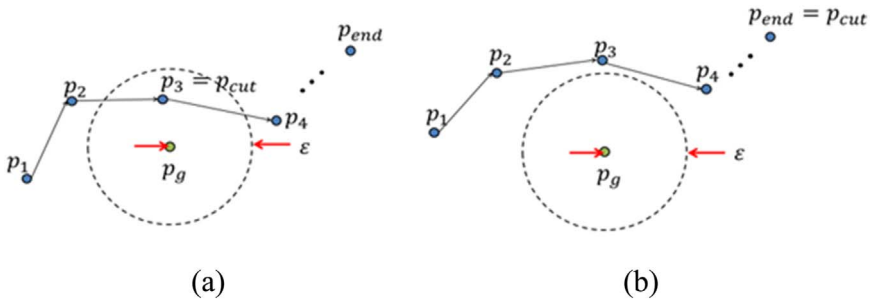

Fig. 6. Example of determination of the last location point.

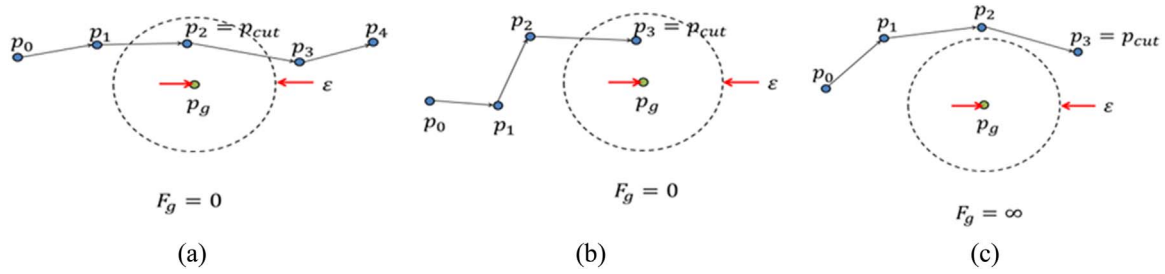

Fig. 7. Examples of the cases when $F_g = 0$ and $F_g = \infty$.

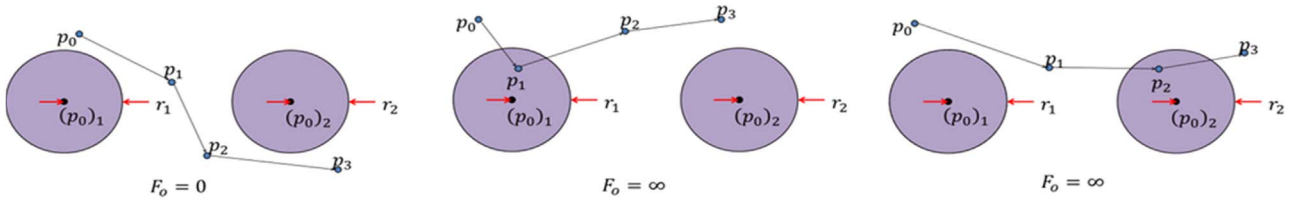

Fig. 8. Examples of the cases when $F_o = 0$ and $F_o = \infty$.

Table 1
Specific techniques and conditions of genetic algorithm used in the simulation.

Genetic operator	Technique
Initialization	Random initialization
Reproduction	Roulette wheel selection
Crossover	One-point crossover with probability 0.8
Mutation	Simple mutation with probability 0.8
Condition	
Resolving power	40
Population size	1000
Termination condition	1000 of generations

Table 2
Coefficients of environmental loads.

Current load		Wind load		Wave load	
ρ	$1025 kg/m^3$	ρ_a	$1.225 kg/m^3$	ρ	$1025 kg/m^3$
A_{Fc}	$2.36 m^2$	A_{Fw}	$2.36 m^2$	g	$9.81 m/s^2$
A_{Lc}	$2.36 m^2$	A_{Lw}	$2.36 m^2$	N	58
C_{Xc}	0.44	C_{Xw}	0.44		
C_{Yc}	0.44	C_{Yw}	0.44		

The weighted values of each objective function are considered equal. The fitness function is derived from the final objective function value using the mapping equation (Eq. (1)).

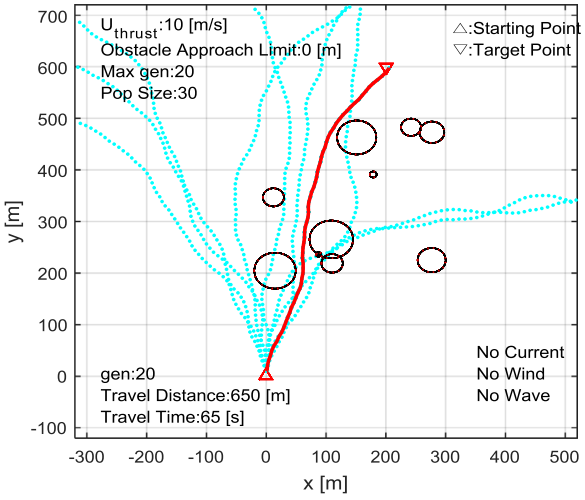

Fig. 9. Optimized path with multi-obstacles.

5. Simulation of an optimized path selection

5.1. Specific techniques and conditions of genetic algorithm used in simulation

The specific techniques and conditions of genetic algorithm used in the simulation are demonstrated in Table 1.

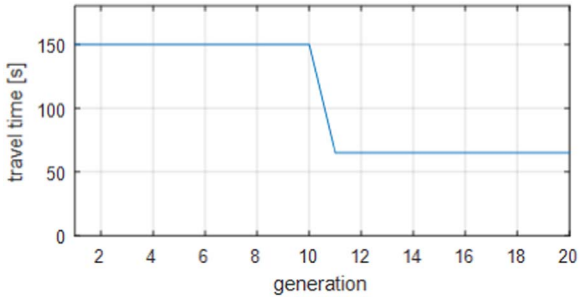

Fig. 10. Travel time for different generations.

5.2. Objective vessel model and environmental loads

The data of an objective vessel is selected from the USV 'Aragon', whose displacement is 2600 kgf. In the simulation, the maneuvering equation of motion of 'Aragon' was simplified as

$$M_{RB}\dot{\nu} = \tau_{current} + \tau_{wind} + \tau_{wave} \tag{13}$$

where M_{RB} is the rigid-body mass matrix, $\dot{\nu}$ is the acceleration vector, and $\tau_{current}$, τ_{wind} and τ_{wave} are the vectors of current force, wind force and wave-induced force, respectively (Fossen, 2011). The ship speed was set to be 10 m/s, and the maximum turning angle was set to be 10 °/sec, based on the motion characteristics of 'Aragon' (Yun et al., 2015). The ship motion for yaw was not taken into account as calculation of the ship motion was simplified to ship speed and turning angle.

The environmental loads include current, wind, and wave forces. The vector of current force is given by

$$\tau_{current} = \begin{bmatrix} X_{current} \\ Y_{current} \end{bmatrix} = \begin{bmatrix} \frac{1}{2}\rho A_{Fc} C_{Xc}(\gamma_{rc}) V_{rc}^2 \\ \frac{1}{2}\rho A_{Lc} C_{Yc}(\gamma_{rc}) V_{rc}^2 \end{bmatrix} \tag{14}$$

where $\tau_{current}$ is the vector of current force, $X_{current}$ and $Y_{current}$ are the current forces during surge and sway, respectively, ρ is the density of water, A_{Fc} and A_{Lc} are the frontal and lateral projected currents areas, respectively, C_{Xc} and C_{Yc} are the current coefficients, γ_{rc} is the relative current angle of attack, and V_{rc} is the relative current speed.

The vector of wind force is given by

$$\tau_{wind} = \begin{bmatrix} X_{wind} \\ Y_{wind} \end{bmatrix} = \begin{bmatrix} \frac{1}{2}\rho_a A_{Fw} C_{Xw}(\gamma_{rw}) V_{rw}^2 \\ \frac{1}{2}\rho_a A_{Lw} C_{Yw}(\gamma_{rw}) V_{rw}^2 \end{bmatrix} \tag{15}$$

where τ_{wind} is the vector of wind force, X_{wind} and Y_{wind} are the wind forces during surge and sway, respectively, ρ_a is the density of air, A_{Fw} and A_{Lw} are the frontal and lateral projected winds areas, respectively, C_{Xw} and C_{Yw} are the wind coefficients, γ_{rw} is the relative wind angle of attack, and V_{rw} is the relative wind speed.

The vector of wave-induced force is given by

$$\tau_{wave} = \tau_{wave1} + \tau_{wave2} \tag{16}$$

$$\tau_{wave1} = \sum_{k=1}^{N} \rho g |F_{wave1}(\omega_k, \beta)| A_k \cos(\omega_e(U, \omega_k, \beta)t + \angle F_{wave1}(\omega_k, \beta) + \epsilon_k) \tag{17}$$

$$\tau_{wave2} = \sum_{k=1}^{N} \rho g |F_{wave2}(\omega_k, \beta)| A_k^2 \cos(\omega_e(U, \omega_k, \beta)t + \epsilon_k) \tag{18}$$

where τ_{wave} is the vector of wave-induced force, τ_{wave1} and τ_{wave1} are the first and second wave forces, respectively, N is the number of harmonic components, ρ is the density of water, g is the acceleration due to gravity, F_{wave1} and F_{wave2} are the force response amplitude operators of the first and second wave forces, respectively, β is the wave encounter angle, ω_e is the encounter frequency, U is the total speed of the ship, t is the time, and ω_k, A_k, and ϵ_k are the wave frequency, wave amplitude, and random phase angle of the k^{th} wave component, respectively.

The coefficients of environmental loads are shown in Table 2.

In Eqs. (17) and (18), the F_{wave1} and F_{wave2} were calculated from RAO of FPSO, which was provided from (Fossen, 2011), with the RAO mapping coefficient as 2.5894×10^{-5}, which was the ratio of displacement. A_k is derived from significant wave height and modal period of modified PM spectrum, which can be set in a simulation.

In this research, environmental load affects moving distance of ship between adjacent points along the created path.

5.3. Simulation result of optimized path section

In this simulation, it was assumed that the obstacles are fixed because this study focused on the path optimization problem for an ENC.

The optimized path with multi-obstacles, and the travel time for different generations are shown in Fig. 9 and Fig. 10, respectively.

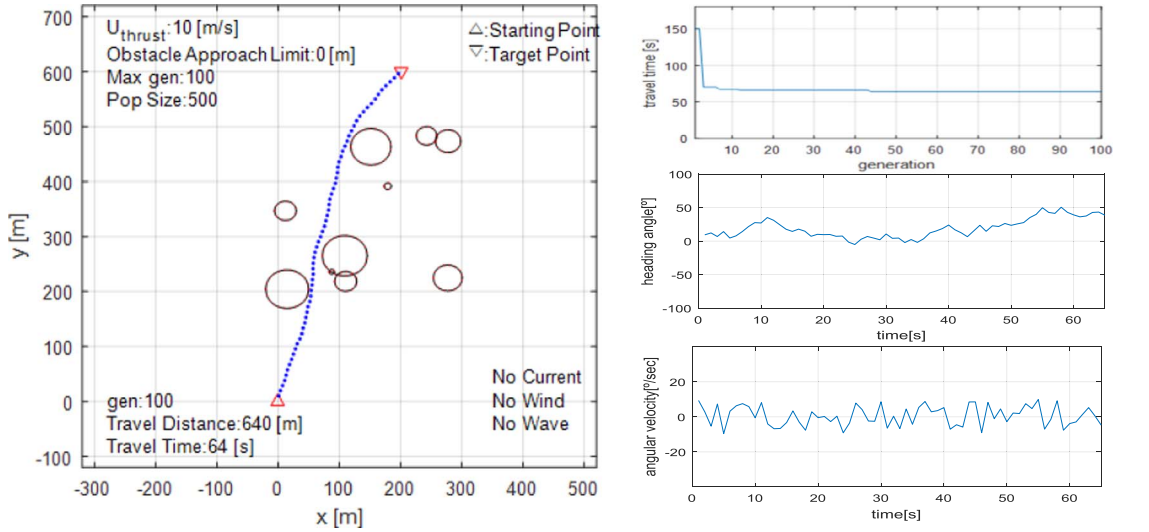

(a) Optimized path

(b) Travel time, heading angle, and angular velocity vs. time

Fig. 11. Optimized path without obstacle approach limit.

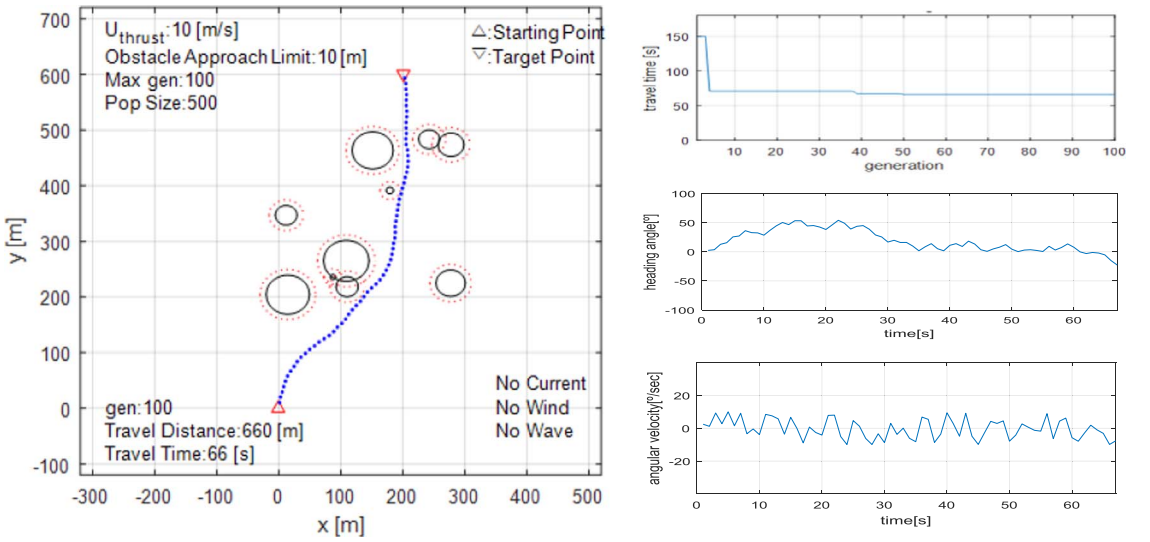

(a) Optimized path

(b) Travel time, heading angle, and angular velocity vs. time

Fig. 12. Optimized path with obstacle approach limit of 10 *m*.

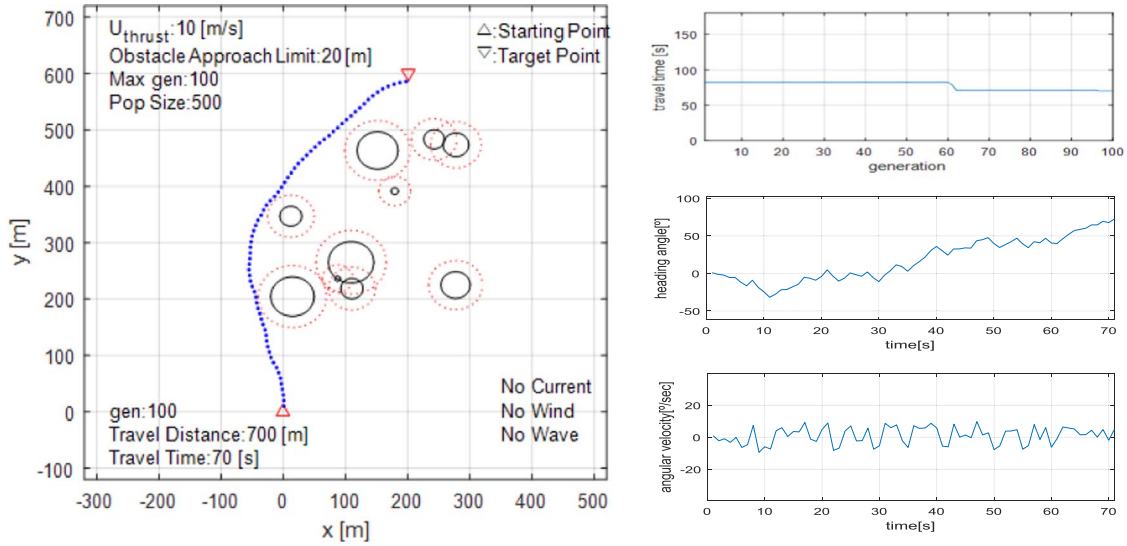

(a) Optimized path

(b) Travel time, heading angle, and angular velocity vs. time

Fig. 13. Optimized path with obstacle approach limit of 20 *m*.

The number of generations should be large in order to obtain a reliable path. However, it was set to be 20 to make the paths of all generations visible. In Fig. 9, the solid line is the final determined path, and the dotted lines are the paths that are generated randomly during the evolution process. The paths that do not reach the target location or pass through the obstacles are excluded at the fitness evaluation stage. At the 11th generation, the optimized path that avoids obstacles and reaches the target location simultaneously is created, as shown in Fig. 10.

Different optimized paths, determined using different obstacle approach limits, are shown in Figs. 11–13.

In this study, in order to consider the crash avoidance caused by the size of the ship, the obstacle approach limits were set to be 0 *m*, 10 *m*, and 20 *m*. If the ship could not create a path between the obstacles due to excessive narrowness, then the paths were created around the obstacles. In the progress of generation going, the candidates of paths are created randomly with spatial equality over the map. Thus, the narrower gaps between obstacles are, the lower survival probability of the paths is during the process. In addition, the proposed algorithm could carry out the optimized path selection by increasing the obstacle approach limit, even if the size of the ship was changed.

Some examples of optimized paths with an obstacle approach limit of 10 *m*, with and without environmental loads, are shown in Fig. 14. The locations and sizes of the obstacles, the significant wave height, and modal period of the wave were set randomly in order to simulate actual environmental conditions. The directions of environmental loads were set to the same degree as an extreme condition in order to show the obvious difference between with and without environmental load. The number of generations was set to be 1000, which was

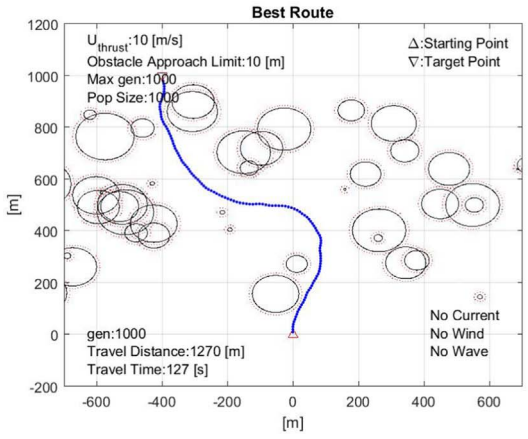

(a) Optimized path without environmental loads

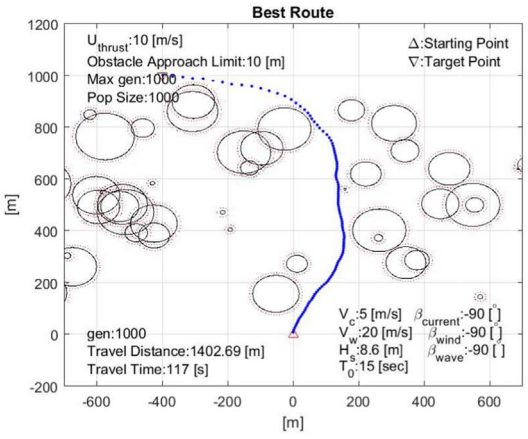

(b) Optimized path under environmental loads with load directions $-90°$

Fig. 14. Optimized path in case 1.

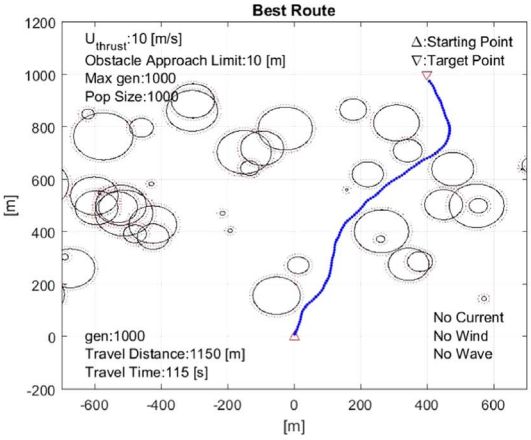

(a) Optimized path without environmental loads

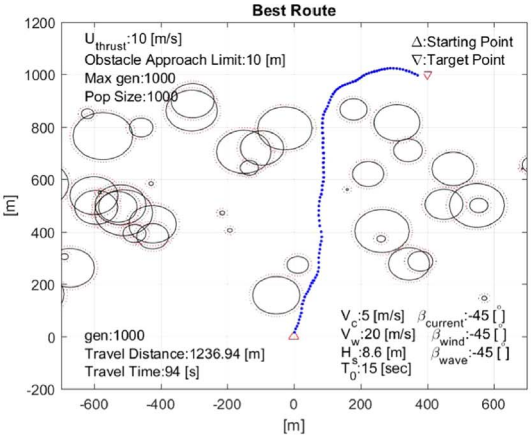

(b) Optimized path under environmental loads with load directions $-45°$

Fig. 15. Optimized path in case 2.

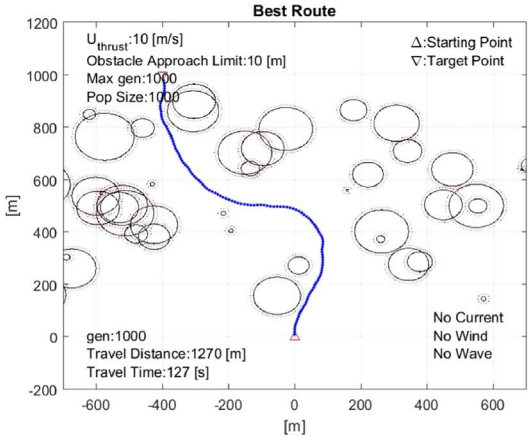

(a) Optimized path without environmental loads

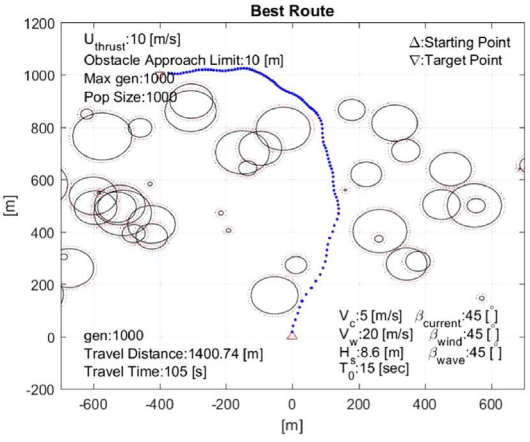

(b) Optimized path under environmental loads with load directions 45°

Fig. 16. Optimized path in case 3.

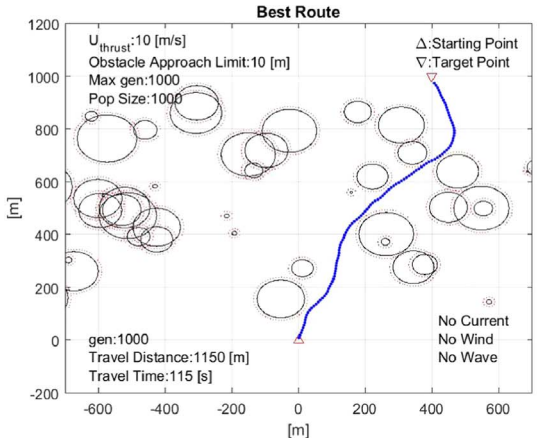

(a) Optimized path without environmental loads

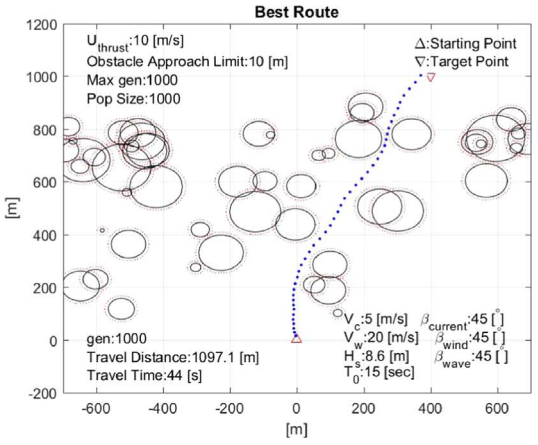

(b) Optimized path under environmental loads with load directions 45°

Fig. 17. Optimized path in case 4.

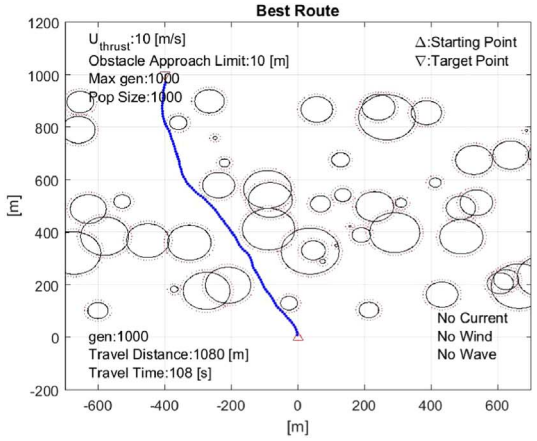

(a) Optimized path without environmental loads

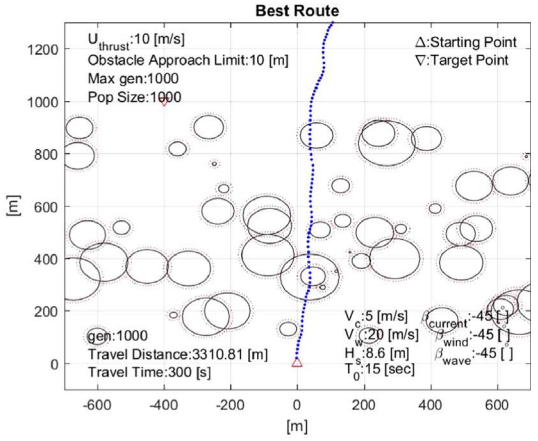

(b) Optimized path under environmental loads with load directions −45°

Fig. 18. Optimized path in case 5.

large enough to converge to the optimum value, in order to obtain a reliable path.

Figs. 14–18 show optimized paths with and without environmental loads with 5 cases. Each of (a) do not include environmental load while each of (b) include environmental load. In the (b) of Fig.s 14–18, the paths were created with shorter travel time comparing to (a), by following the direction of environmental loads. In the (b) of Fig. 18, it shows the case that path cannot be created due to the lack of thrust capacity to overcome environmental load. The environmental loads cause a change in the ship's speed. Thus, the paths were created as not the shortest distance route, but the shortest time route that follows dominant environmental loads.

The following processor and software were used for carrying out the simulations: Intel(R) Core(TM) i5-6600 CPU-3.30 GHz, Windows 8, and MATLAB 2015a. The time required for the simulations to complete was approximately 30 min, without parallel computing, when the population size was 1000 and the number of generations was 1000. Parallel computing is necessary to reduce the computing time for the proposed algorithm.

6. Result and discussions

In this study, a path optimization method using a genetic algorithm was proposed for a ship, considering environmental loads, obstacle avoidance, and minimization of travel time. Additionally, fitness functions were defined for avoiding obstacles, reaching a target location, and minimizing travel time. The optimized paths were derived by repeating the fitness evaluation of chromosomes over all generations, based on the fitness functions.

The conclusions drawn from this research are as follows:

First, all the paths that are created over all generations are

evaluated based on the fitness. Then, new paths are created through the processes of the genetic operators. The paths that have low fitness become extinct during the processes, and the processes are repeated until the stopping criteria are reached.

Second, the optimized paths that are safe from collision are determined by setting the obstacle approach limit even if environmental disturbance is uncertain. The paths are created around the obstacles if the path of the ship between the obstacles is excessively narrow. This situation was simulated in this research.

Third, the optimized paths considering the dominant environmental loads are determined in order to minimize the travel time over the evolution process. The environmental loads cause a change in the ship's speed. This situation was simulated in this research.

The recommended next step is to carry out research considering 6 degrees of freedom. Further, a real-time path optimization algorithm can be developed using the data of moving obstacles and ships.

Acknowledgement

This work is supported by the Inha University (Research Project Number: 52752).

References

Fossen, T.I., 2011. Handbook of marine craft hydrodynamics and motion control= : Vademecum de Navium Motu Contra Aquas et de Motu Gubernando, Hoboken, N.J., Wiley ; Chichester : John Wiley [distributor].

Jin, G.-G., 2010. Genetic Algorithm and Their applications, Seoul, KyoWooSa.

Kim, H., Myung, H., So, N.-S., 2012. Development of path planning algorithm for an autonomous navigation of an unmanned surface vehicle. Soc. Nav. Archit. Korea, 514–517.

Lee, B.-K., Kim, J.-H., Kim, D.-Y., Kim, T.-H., 2000. A Study on the Optimal Trajectory Planning for a Ship Using Genetic algorithm. Institute of Control, Robotics and Systems, 2112–2115.

Lee, K.-Y., Kim, S., Song, C.-H., 2012. Global path planning for autonomous underwater vehicles in current field with obstacles. J. Ocean Eng. Technol. 26, 1–7.

Yun, K.H., Kim, D.J., Son, N.S., Kim, S.Y., 2015. A study on the algorithm of target tracking system for usv based on simulation method. J. Ships Ocean Eng. 56, 19–25.